JOURNAL OF AIRCRAFT
Vol. 47, No. 6, November–December 2010

Engineering Notes

Minimizing Induced Drag with Spanwise Blowing Variation on a Circulation-Controlled Wing

N. R. Alley*
Aerotonomy, Incorporated, Lithia Springs, Georgia 30122
and
W. F. Phillips†
Utah State University, Logan, Utah 84322-4130

DOI: 10.2514/1.C001010

Nomenclature

A_j	=	jet slot area
b_w	=	wingspan
C_{Di}	=	induced drag coefficient
C_L	=	wing lift coefficient
C_{L_d}	=	design lift coefficient
C_μ	=	blowing coefficient (momentum coefficient) $2\rho_j A_j V_j^2/\rho_\infty V_\infty^2 S_w$
$\tilde{C}_\mu$	=	local airfoil section blowing coefficient (momentum coefficient) $2\rho_j h_j V_j^2/\rho_\infty V_\infty^2 c$
$\tilde{\mathbf{C}}_\mu$	=	local airfoil section blowing coefficient vector
c	=	local airfoil section chord length
h_j	=	jet slot height
m	=	number of spanwise jet-boundary sections
n	=	number of spanwise control points
S_w	=	wing planform area
V_∞	=	magnitude of the freestream velocity
V_J	=	magnitude of the jet-exit velocity (determined from isentropic relations)
y^+	=	shear Reynolds number for the grid layer next to the airfoil or wing surface
Δ	=	modifier indicating an incremental change
ρ_∞	=	freestream air density
ρ_j	=	jet-exit air density
∇	=	gradient modifier

I. Introduction

THE purpose of the work described here was to investigate a combination of existing technologies that could allow an aircraft to fly efficiently in both the high- and low-speed regimes. These technologies are the *twisteron* [1] and the *circulation-controlled wing* [2].

Phillips et al. [1] have shown that an unswept wing of any planform shape can be controlled to reduce induced drag to an absolute minimum through the use of flexible trailing-edge flaps, which were called twisterons. These trailing-edge flaps can be continuously adjusted during flight so that the wing always operates at the optimal lift distribution, which results in minimum induced drag.

Circulation-controlled (CC) wings make use of the *Coanda effect* [3] to maintain attached flow at high-lift coefficients by blowing a small, high-velocity jet sheet over a highly curved trailing edge. Because the trailing edge of a CC airfoil is not sharp, the Kutta condition is not fixed, but set by the amount of blowing. With increased blowing, the front and rear stagnation points move toward the lower surface of the airfoil to provide increased circulation and, hence, increased lift [4]. Using the Coanda effect to generate high-lift coefficients has been studied since the 1930s and has been implemented successfully on two demonstration aircraft [5,6]. These aircraft were able to generate two to three times the lift generated by comparable conventional aircraft in high-lift configurations. This resulted in a significant increase in short takeoff and landing (STOL) capabilities. However, the copious amounts of induced drag generated at such high-lift coefficients precluded the efficient use of CC wings in low-speed cruising flight and their rounded trailing edges resulted in poor performance during high-speed cruise.

The latter problem of poor performance at high-speed cruise was solved by the advent of the advanced CC wing, which has a rounded Coanda surface that can be retracted when not in use [7,8]. However, high induced drag levels continue to limit the use of CC lift augmentation to improving STOL performance.

The present work describes a method for reducing the induced drag generated on a CC wing by varying the blowing along the span of the wing so that an optimum lift distribution is obtained. This blowing distribution could be varied with flight conditions to minimize induced drag. Although induced drag levels would still be significant, pneumatic twisterons could also allow an aircraft to fly as efficiently as possible at very low velocities. An aircraft implementing this technology would be capable of flying efficiently in both the low- and high-speed flight regimes.

The geometric twisterons proposed by Phillips et al. [1] use spanwise variations in flap deflection to minimize the induced drag generated on a conventional wing. It was hypothesized that similar drag reductions might be achieved for a CC wing by implementing spanwise variations in blowing strength [9]. Thus, it was the purpose of the present work to determine whether or not a spanwise blowing distribution could be obtained that minimized the induced drag generated on a CC wing.

Although a closed-form solution exists that defines the drag-minimizing twist distributions for conventional unswept wings [1], no such solutions exist that describe the blowing distributions that would minimize the induced drag generated on a CC wing. Hence, the drag-minimizing blowing distribution must be obtained either experimentally or using computational fluid dynamics (CFD). Here, the results of a CFD optimization study are presented. Analogous to conventional wings, the optimal blowing distributions on a CC wing will vary with wing shape and flight conditions. For example, results are presented here for a rectangular CC wing with a 15% thick elliptic airfoil and an aspect ratio of 20. For the example presented, the blowing distribution is optimized for an operating lift coefficient of 1.0.

Hundreds of CFD simulations of various flows about CC airfoils and wings were performed. The results were employed to develop the CFD model that was used to simulate the drag-minimizing blowing distributions. This CFD model was coupled with an optimization algorithm that iteratively adjusted the blowing distributions within the CFD model until a drag-minimized solution was found.

Presented as Paper 2007-711 at the 45th AIAA Aerospace Sciences Meeting and Exhibit, Reno, NV, 8–11 January 2007; received 8 March 2010; revision received 22 June 2010; accepted for publication 25 June 2010.

*Chief Technology Officer, 591 Thornton Rd. Suite A. Member AIAA.
†Professor, Mechanical and Aerospace Engineering Department, 4130 Old Main Hill. Senior Member AIAA.

II. Computational Fluid Dynamic Simulations

All CFD flow simulations were performed using version 6.4 of the computational fluid dynamics code CFL3D [10]. The flow solver CFL3D is a structured-grid, multizone code that solves the three-dimensional, time-dependent, Reynolds-Averaged Navier–Stokes (RANS) equations using an upwind finite-volume formulation. Local time stepping, mesh sequencing, and low-Mach-number preconditioning were used. Converged solutions were defined by a reduction in the norm of the density vector residual of at least 3 orders of magnitude and asymptotic convergences of both lift and drag coefficients.

It was expected that hundreds of three-dimensional CFD simulations would be required to obtain a spanwise blowing distribution that minimized induced drag. Reducing this computational expense would require that the 3-D grids be as coarse as possible without sacrificing stability, physical accuracy, or grid resolution. Additionally, of the hundreds of 3-D cases ran during the final analyses, it was imperative that each yielded converged solutions. Of equal importance was that the turbulence model be extremely stable and robust in modeling the Coanda effect over a wide range of blowing coefficients.

For the 3-D simulations, the Reynolds number was kept constant while the simulated freestream temperature, density, and viscosity were set to 15°C, 1.225 kg/m^3, and 1.73×10^{-5} N.s/m^2 [2], respectively. This resulted in a velocity of approximately 20 mph and a Mach number of 0.023. The angle of attack was continuously adjusted to maintain a specified lift coefficient. The wing boundary was modeled as an adiabatic viscous surface and the jet characteristics at the Coanda-jet boundary were specified using the isentropic relations and set using an inflow boundary condition that required the specification of the jet Mach number, the ratio of the jet total pressure to the freestream pressure, and the ratio of the jet total temperature to the freestream temperature. A turbulence level yielding an eddy viscosity of 0.009 was used for the freestream and jet inflows.

It was known that the most robust turbulence model would not necessarily be the most accurate. The ability of the turbulent solution to reproduce physical trends (i.e., increased blowing results in increased circulation) and its stability were given priority over matching experimental data exactly. In Alley [9] and Alley et al. [11], a 2-D analysis was performed where the wind-tunnel experiments on a 15% thick elliptic CC airfoil [12] were reproduced using each of the turbulence models available in version 6.4 of CFL3D. The Spalart–Allmaras model [13] was found to be the most robust while consistently reproducing well-resolved and physically accurate results over a wide range of blowing coefficients. However, it is the belief of the authors that further work is required in the area of turbulence modeling before the RANS equations can reproduce, with exactness, the flows through the free shear layers and about the highly curved surfaces characteristic of the Coanda effect.

A CC wing with symmetric, 15% thick elliptic airfoil cross sections and an aspect ratio of 20 was selected. Nearly 100 distinct CFD mesh representations of this wing were created, one of which can be seen in Fig. 1. Mesh effect studies were performed where boundary sizes, nodal distributions, and nodal densities were all adjusted to generate a grid that provided stable, computationally efficient, and well-resolved solutions throughout the required range of operating conditions.

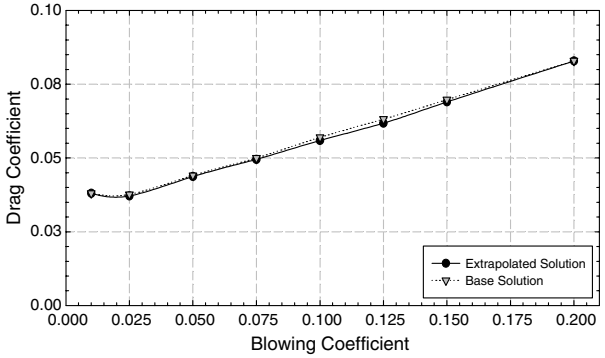

Fig. 2 Grid resolution for the drag predicted from three-dimensional solutions.

Numerical simulations of the CC wing at the test lift coefficient were performed for uniform spanwise blowing distributions with a range of blowing coefficients from 0.01 to 0.20. Richardson extrapolations of the multigrid solutions [14–16] were used to measure grid resolution. The base drag coefficients were compared with their extrapolations, as grid resolution is indicated by an extrapolated solution that is close to, or matches, the base solution. The grid resolution of the final grid is illustrated in Fig. 2, which shows excellent agreement between extrapolated and base solutions. The final grid consistently produced well-resolved and physically realistic solutions for all test conditions and the iteration-convergence plots for each test solution, without exception, showed excellent stability. This grid contained 107 normal-nodal levels extending radially away from the wing surface and 225 nodes along the circumference of the airfoil sections with 104 of the 225 nodes located aft of the Coanda jet. A wing generated with 49 spanwise sections that were spaced with cosine clustering to add refinement near the wingtips was found to be the most computationally efficient while maintaining grid resolution. The boundary layer was refined until an average y^+ value of approximately 1.0 was obtained for the surface boundary elements.

III. Optimization Procedure

A method was developed for determining the blowing distribution that minimizes the induced drag generated on a CC wing at some design lift coefficient, C_{L_d}. Using CFD, a variable blowing distribution was obtained by discretizing the Coanda-jet boundary on the wing into m spanwise sections and allowing the blowing to vary from section to section. By holding the lift coefficient constant through varying the angle of attack, the induced drag becomes a

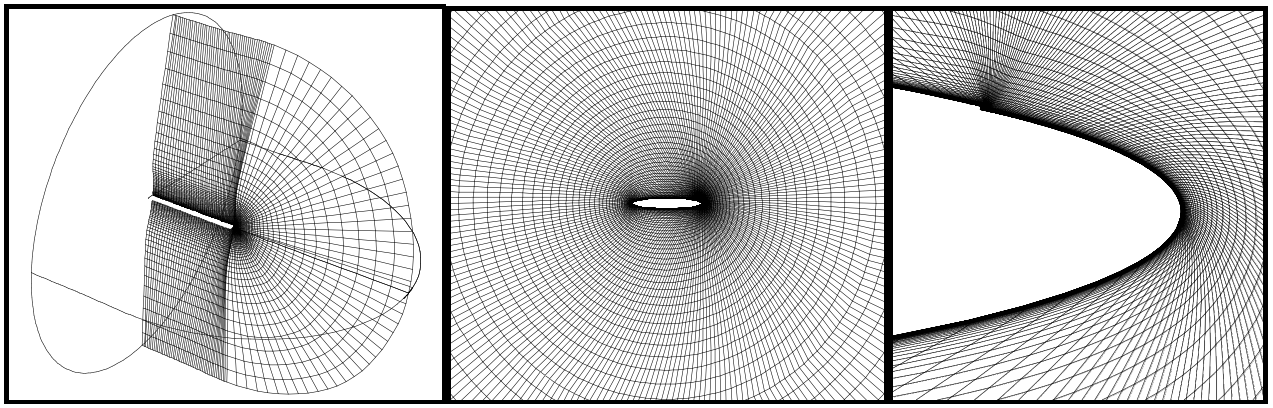

Fig. 1 From left to right; example of a 3-D 20-chord grid generated about a CC wing, 2-D slice showing grid generated about an elliptic airfoil, closeup 2-D view of Coanda jet and Coanda surface.

function of blowing strength at each section. This induced drag is minimized when the blowing distribution is such that the gradient of the induced drag with respect to the blowing becomes zero:

$$\nabla C_{D_i}(\tilde{C}_{\mu_1}, \tilde{C}_{\mu_2}, \ldots \tilde{C}_{\mu_m})_{C_L = C_{L_d}} = 0 \tag{1}$$

Given that induced drag is a nonlinear function of blowing strength, an algorithm capable of solving this m-dimensional, nonlinear equation had to be implemented.

Various multidimensional optimization methods were evaluated with the steepest descent [17] and Broyden–Fletcher–Goldfarb–Shanno (BFGS) methods [18] being found to be the most appropriate. The initial iterations were stabilized by using the steepest descent method as it was able to reduce the large initial gradients that were problematic for the BFGS method. After several iterations, the solutions were such that the BFGS method could be implemented and run to convergence without incident.

To reduce the calculations required to compute the gradient, the blowing strength at each of the m spanwise boundary sections was estimated using a cubic spline interpolation of n, cosine-distributed control points. An algorithm using the optimization methods coupled with a blowing-interpolation routine was developed, which was coupled with various shell scripts to allow it to operate and collect the three-dimensional CFD results from CFL3D. The flow solver, CFL3D, was used to compute the base solution and gradients for a given blowing distribution. The gradient values were then used by the optimization algorithm to generate a new blowing distribution, which was again solved using CFL3D to find its gradients. This iterative process was repeated until an optimized solution was obtained. Optimization was monitored through the total gradient or the average of the absolute values of the gradients. When the total gradient had been reduced by 3 orders of magnitude the solution was considered to be optimized.

The jet boundary of the 3-D grid was broken up into 24 spanwise sections. To reduce the number of CFD runs required per iteration, the blowing strength at each of the 24 sections was estimated using a cubic-spline interpolation with five, cosine-distributed control points. Using the central difference method, the gradient as defined by Eq. (1), was approximated by,

$$\nabla C_{D_i}(\tilde{\mathbf{C}}_\mu) \cong \begin{bmatrix} \frac{C_{D_i}(\tilde{C}_{\mu_1}+\Delta C_\mu, \tilde{C}_{\mu_2}, \tilde{C}_{\mu_3}, \tilde{C}_{\mu_4}, \tilde{C}_{\mu_5}) - C_{D_i}(\tilde{C}_{\mu_1}-\Delta C_\mu, \tilde{C}_{\mu_2}, \tilde{C}_{\mu_3}, \tilde{C}_{\mu_4}, \tilde{C}_{\mu_5})}{2\Delta C_\mu} \\ \frac{C_{D_i}(\tilde{C}_{\mu_1}, \tilde{C}_{\mu_2}+\Delta C_\mu, \tilde{C}_{\mu_3}, \tilde{C}_{\mu_4}, \tilde{C}_{\mu_5}) - C_{D_i}(\tilde{C}_{\mu_1}, \tilde{C}_{\mu_2}-\Delta C_\mu, \tilde{C}_{\mu_3}, \tilde{C}_{\mu_4}, \tilde{C}_{\mu_5})}{2\Delta C_\mu} \\ \frac{C_{D_i}(\tilde{C}_{\mu_1}, \tilde{C}_{\mu_2}, \tilde{C}_{\mu_3}+\Delta C_\mu, \tilde{C}_{\mu_4}, \tilde{C}_{\mu_5}) - C_{D_i}(\tilde{C}_{\mu_1}, \tilde{C}_{\mu_2}, \tilde{C}_{\mu_3}-\Delta C_\mu, \tilde{C}_{\mu_4}, \tilde{C}_{\mu_5})}{2\Delta C_\mu} \\ \frac{C_{D_i}(\tilde{C}_{\mu_1}, \tilde{C}_{\mu_2}, \tilde{C}_{\mu_3}, \tilde{C}_{\mu_4}+\Delta C_\mu, \tilde{C}_{\mu_5}) - C_{D_i}(\tilde{C}_{\mu_1}, \tilde{C}_{\mu_2}, \tilde{C}_{\mu_3}, \tilde{C}_{\mu_4}-\Delta C_\mu, \tilde{C}_{\mu_5})}{2\Delta C_\mu} \\ \frac{C_{D_i}(\tilde{C}_{\mu_1}, \tilde{C}_{\mu_2}, \tilde{C}_{\mu_3}, \tilde{C}_{\mu_4}, \tilde{C}_{\mu_5}+\Delta C_\mu) - C_{D_i}(\tilde{C}_{\mu_1}, \tilde{C}_{\mu_2}, \tilde{C}_{\mu_3}, \tilde{C}_{\mu_4}, \tilde{C}_{\mu_5}-\Delta C_\mu)}{2\Delta C_\mu} \end{bmatrix}_{C_L = C_{L_d}} \tag{2}$$

where ΔC_μ is the differential step size, which was set to 1×10^{-6}. As illustrated in Eq. (2), each numerical calculation of the gradient required ten CFD runs per iteration.

Iterations began with a uniform blowing distribution set to a C_μ of 0.1. The initial 3-D analysis showed that a uniform blowing coefficient of 0.1 resulted in a zero-angle-of-attack wing lift coefficient of approximately 1.7. It was decided that the lift coefficient resulting from this uniform blowing distribution was far enough removed from the test lift coefficient that the optimized solution would not be influenced by this initial distribution.

IV. Results

The optimized blowing distribution for a lift coefficient of 1.0 was found for a rectangular CC wing with 15% thick elliptic airfoils and an aspect ratio of 20. Starting from a uniform distribution, the blowing was optimized using a combination of the steepest descent and BFGS methods. The convergence of the blowing distributions

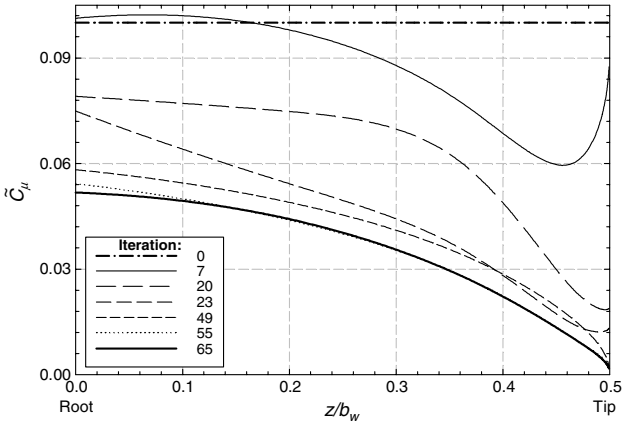

Fig. 3 Blowing distribution convergence.

and drag coefficients are shown in Figs. 3 and 4, respectively. These figures show that after 55 iterations the solution was essentially converged as the induced drags and blowing distributions of the 55th and 65th iterations are nearly identical.

Figure 4 shows that the initial induced drag coefficient of 0.0296 was reduced by 25% to an optimized value of 0.0222. Although the optimization in this study was based solely on reducing the induced drag, if the viscous drag were to increase as the induced drag was minimized, the overall benefit of the optimization would diminish or be nullified. Therefore the viscous drag was analyzed as well, and the iterative convergence of the viscous drag is also plotted in Fig. 4. This figure illustrates a secondary benefit of optimizing the blowing distribution; i.e., the reduction in induced drag is accompanied by a corresponding reduction in viscous drag. Because of this decreases in viscous drag, the optimization achieved a 32% reduction in total drag.

The viscous drag reduction is due likely to the corresponding reductions in blowing magnitude seen over the span of the wing (see Fig. 3). The Coanda jet exhaust and resulting flow entrainment tends

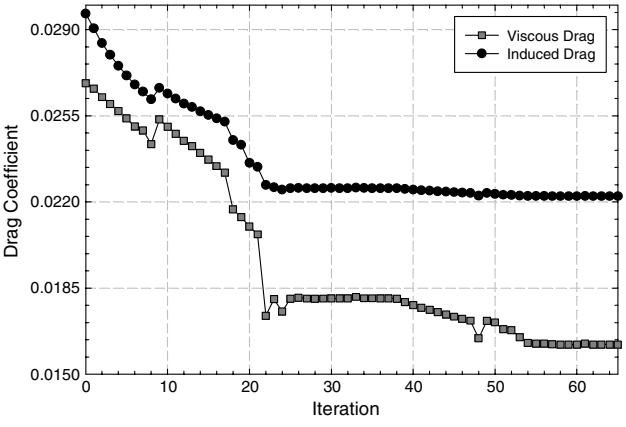

Fig. 4 Viscous and induced drag convergences.

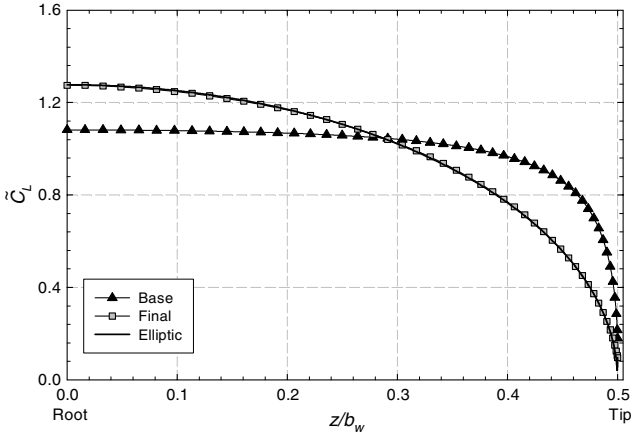

Fig. 5 Initial and optimized lift distributions.

to increase the average flow velocity near the surface of the airfoil. Therefore reducing the blowing magnitude would reduce the average surface flow velocity, which would, in turn, reduce the overall viscous drag.

The foundation of the optimization process described here lies in achieving the lift distribution that most efficiently sheds the vorticity generated by a finite wing, thus reducing the induced drag to its absolute minimum. Such drag minimization on a conventional rectangular wing can be achieved by adjusting a full-span trailing-edge flap, or twisteron [1], in such a manner that the spanwise lift distribution becomes elliptic. Because the purpose of this work was to develop the pneumatic equivalent of a geometric twisteron, the shape of the drag-minimizing lift distribution is of interest.

The initial lift distribution and that of the final optimized solution are shown in Fig. 5. The optimized blowing distribution was found to generate an elliptic lift distribution. For comparison, Fig. 5 also includes the elliptic lift distribution that results in a wing lift coefficient equaling the test lift coefficient. It should be noted that the BFGS optimization algorithm affords no way to know with mathematical certainty that the optimized solution obtained in this work is a global optimum. However, the fact that the optimized blowing distribution produced a near perfect elliptic lift distribution provides additional evidence that the global optimum had been reached.

To ensure that an accurate comparison of the effectiveness of optimized spanwise blowing, a final test case was run using a uniform blowing distribution having the same overall magnitude as the optimized blowing distribution (see Fig. 6). At the test lift coefficient, the induced drag generated by the optimized blowing distribution was found to be 11% lower than that generated by the equivalent uniform distribution. The optimized distribution also showed a slight

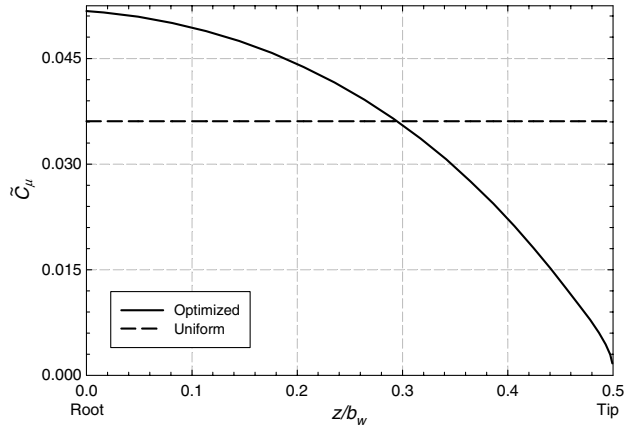

Fig. 6 Uniform and optimized blowing distributions of equal magnitude.

reduction in viscous drag, which resulted in a total drag reduction of 6.5%. Finally, the optimized distribution was found to be 2.4% more effective at lift generation, as the uniform distribution was found to require a higher angle of attack to attain the test lift coefficient of 1.0.

V. Conclusions

Results presented here show that minimizing induced drag on a CC wing through changes in the spanwise blowing distribution can be very effective. Using computational fluid dynamics, an optimized blowing distribution at a lift coefficient of 1.0 was found for a rectangular circulation-controlled wing with 15% thick elliptic airfoils and an aspect ratio of 20. Starting from a uniform distribution, the blowing was optimized using a combination of the steepest descent and BFGS methods. The optimized blowing distribution was found to generate an elliptic lift distribution. Induced drag was reduced by more than 11% and the total drag was reduced by 6.5% from that generated by an equivalent uniform blowing distribution.

Acknowledgments

Most of the computations for this work were performed on the Uinta supercomputer, which was provided by the National Science Foundation under grant number CTS-0321170 with matching funds provided by Utah State University. The authors would like to acknowledge the computer time donated by the Center for High Performance Computing at Utah State University.

References

[1] Phillips, W. F., Alley, N. R., and Goodrich, W. D., "Lifting-Line Analysis of Roll Control and Variable Twist," *Journal of Aircraft*, Vol. 41, No. 5, 2004, pp. 1169–1176. doi:10.2514/1.3846

[2] Englar, R. J., "Circulation Control Pneumatic Applications: Blown Force and Moment Augmentation and Modification; Past, Present, and Future," AIAA Paper 2000-2541, June 2000.

[3] Metral, A. R., "On the Phenomenon of Fluid Veins and Their Application, the Coanda Effect," United States Air Force F-TS-786-RE, 1939.

[4] Williams, S. L., and Franke, M. E., "Navier–Stokes Methods to Predict Circulation Control Airfoil Performance," *Journal of Aircraft*, Vol. 29, No. 2, 1992, pp. 243–249. doi:10.2514/3.46151

[5] Loth, J. L., Fanucci, J. B., and Roberts, S. C., "Flight Performance of a Circulation Controlled STOL Aircraft," *Journal of Aircraft*, Vol. 13, No. 3, 1976, pp. 169–173. doi:10.2514/3.58647

[6] Englar, R. J., Hemmerly, R. A., Moore, W. H., Seredinsky, V., Valckenaere, W., and Jackson, J. A., "Design of the Circulation Control Wing STOL Demonstrator Aircraft," *Journal of Aircraft*, Vol. 18, No. 1, 1981, pp. 51–58. doi:10.2514/3.57463

[7] Englar, R. J., and Huson, G. G., "Development of Advanced Circulation Control Wing High-Lift Airfoils," *Journal of Aircraft*, Vol. 21, No. 7, 1984, pp. 476–483. doi:10.2514/3.44996

[8] Englar, R. J., Smith, M. J., Kelley, S. M., and Rover, R. C., "Application of Circulation Control to Advanced Subsonic Transport Aircraft, Part I: Airfoil Development," *Journal of Aircraft*, Vol. 31, No. 5, 1994, pp. 1160–1168. doi:10.2514/3.56907

[9] Alley, N. R., "Development of the Pneumatic Twisteron through the Use of Circulation Control Technology," Ph.D. Dissertation, Utah State University, June 2006.

[10] Krist, S. L., Biedron, R. T., and Rumsey, C. L., "CFL3D Users Manual (Version 5)," NASA TM-1998-208444, June 1998.

[11] Alley, N. R., Phillips, W. F., and Spall, R. E., "Minimizing Induced Drag with Blowing Variation along the Span of a Circulation-Controlled Wing," AIAA Paper 2007-711, Jan. 2007.

[12] Englar, R. J., "Two-Dimensional Subsonic Wind Tunnel Tests of Two 15-Percent Thick Circulation Control Airfoil," Naval Ship Research and Development Center AL-211(AD900-210L), Bethesda, MD, Aug. 1971.

[13] Spalart, P., and Allmaras, S., "A One-Equation Turbulence Model for Aerodynamic Flows," *La Recherche Aerospatiale: Bulletin Bimestriel*

de l'Office National d'Etudes et de Recherches Aerospatiales, Vol. 1, No. 1, 1994, pp. 5–21.

[14] Richardson, L. F., "The Approximate Arithmetical Solutions by Finite Differences of Physical Problems Involving Differential Equations, with an Application to the Stresses in a Masonry Dam," *Philosophical Transactions of the Royal Society of London, Series A: Mathematical and Physical Sciences*, Vol. 210, 1910, pp. 307–357.

[15] Richardson, L. F., and Gaunt, J. A., "The Deferred Approach to the Limit," *Philosophical Transactions of the Royal Society of London, Series A: Mathematical and Physical Sciences*, Vol. 226, 1927, pp. 299–361.

[16] Celik, I. B., "Procedure for Estimation and Reporting of Discretization Error in CFD Applications," *Journal of Fluids Engineering*, Editorial policy statement on the control of numerical accuracy, 2006.

[17] Heath, M. T., "Optimization: Secant Updating Methods," *Scientific Computing*, 2nd ed., McGraw–Hill, New York, 2002, pp. 281–283.

[18] Shanno, D. F., "Summary: A New Algorithm for Unconstrained Optimization," *Journal of Optimization Theory and Applications*, Vol. 46, No. 1, 1985, pp. 87–94.
doi:10.1007/BF00938762